Electronic Layer Decoupling Driven by Density-Wave Order in $La_4Ni_3O_{10}$

Ziqiang Guan (管梓强),[1,*] Sophia F. R. TenHuisen,[1,2,*] M. Tepie,[1] Yifeng Zhao (赵祎峰),[3] Ezra Day-Roberts,[3] Harrison LaBollita,[3] Alexander M. Young,[1] Xiaomeng Cui (崔宵萌),[1] Xinglong Chen (陈幸龙),[4] Filippo Glerean,[1,5] Carl Audric Guia,[1] Mark P. M. Dean,[5] Philip Kim,[1,2] J. F. Mitchell,[4] Antia S. Botana,[3] Christopher C. Homes,[6] and Matteo Mitrano[1,†]

[1]*Department of Physics, Harvard University, Cambridge, Massachusetts 02138, USA*
[2]*John A. Paulson School of Engineering and Applied Sciences, Harvard University, Cambridge, Massachusetts 02138, USA*
[3]*Department of Physics, Arizona State University, Tempe, Arizona 85287, USA*
[4]*Materials Science Division, Argonne National Laboratory, Lemont, Illinois 60439, USA*
[5]*Condensed Matter Physics and Materials Science Department, Brookhaven National Laboratory, Upton, New York 11973, USA*
[6]*National Synchrotron Light Source II, Brookhaven National Laboratory, Upton, New York, USA*

(Received 13 January 2026; accepted 28 April 2026; published 26 May 2026)

We probe the density-wave transition of the trilayer nickelate $La_4Ni_3O_{10}$ with polarization-resolved infrared spectroscopy. The low-energy electrodynamics is strongly anisotropic, with metallic in-plane and insulating out-of-plane character. In the ordered phase, the anisotropy grows more than an order of magnitude as the out-of-plane conductivity is sharply suppressed. We interpret this enhancement as an effective electronic decoupling of the Ni-O layers driven by a spin-density-wave-induced redistribution of Ni-d_{z^2} occupation within the trilayers. This electronic response is accompanied by clearly shifting and splitting out-of-plane phonons, compatible with a density-wave instability of electronic origin.

DOI: 10.1103/qgl1-zh9f

Bilayer $La_3Ni_2O_7$ and trilayer $La_4Ni_3O_{10}$ Ruddlesden-Popper (RP) nickelates become superconductors under pressure [1–9]. In both of these materials, superconductivity emerges from density-wave (DW) ground states at ambient pressure, seemingly emulating the phenomenology of hole-doped copper oxides [10–15]. However, unlike high-T_c cuprates, whose low-energy physics is often captured by a single $d_{x^2-y^2}$ band, RP nickelates are multiorbital systems with substantial interlayer coupling. It is, therefore, crucial to resolve how the active orbitals contribute to the DW instabilities, mediate coupling between Ni-O planes, and influence the transport properties of these materials [9,16,17].

The trilayer RP compound $La_4Ni_3O_{10}$, shown in Fig. 1(a), is a compelling platform to address these multiorbital effects. This material has an average Ni valence of $3d^{7.33}$, and both $d_{x^2-y^2}$ and d_{z^2} orbitals contribute to its low-energy physics [18–23]. While $d_{x^2-y^2}$ orbitals are key to the in-plane physics, d_{z^2} states couple the three NiO_3 octahedral layers via apical oxygen hybridization. This out-of-plane coupling also differentiates inner (light purple) and outer (dark purple) Ni-O layers due to their distinct local electronic environments [21,23–25]. At ambient pressure, $La_4Ni_3O_{10}$ exhibits an intertwined spin- and charge-density-wave (SDW, CDW) transition near $T_{DW} \approx 140$ K. The CDW is in phase across all three layers, while the SDW resides on the two antiferromagnetically coupled outer layers, leaving a node in the inner layer [13,17,21,26]. Under pressure, CDW and SDW states collapse, with superconductivity appearing at $T_c \approx 20$–40 K [3,6,14].

In this Letter, we use infrared spectroscopy to investigate how the DW phase influences the low-energy electrodynamics in trilayer nickelate $La_4Ni_3O_{10}$ bulk single crystals. Details on single-crystal sample growth, optical measurements, and computational simulations can be found in the Supplemental Material (SM) [27]. We observe a pronounced electronic anisotropy at far-infrared frequencies, as the in-plane conductivity is metallic, while the conductivity in the out-of-plane stacking c^* direction is insulating. Across the DW transition, the out-of-plane transport is strongly suppressed, yielding an order-of-magnitude enhancement of the transport anisotropy. We attribute this effect to a DW-driven redistribution of Ni d_{z^2} orbital occupation that effectively decouples the Ni-O layers. We also observe distinct phonon renormalizations and mode splittings, consistent with the presence of electron-phonon and magnetoelastic coupling. Together, these results show that the DW phase dramatically reshapes the normal-state properties of RP nickelates.

Figure 1(b) shows the polarized infrared reflectivity of $La_4Ni_3O_{10}$ for in-plane ($E \| ab$) and out-of-plane ($E \| c^*$) directions over a broad frequency range. Here, c^* denotes the direction normal to the ab-plane, which is slightly tilted relative to the crystallographic c axis in the monoclinic $P2_1/a$

*These authors contributed equally to this work.
†Contact author: mmitrano@g.harvard.edu

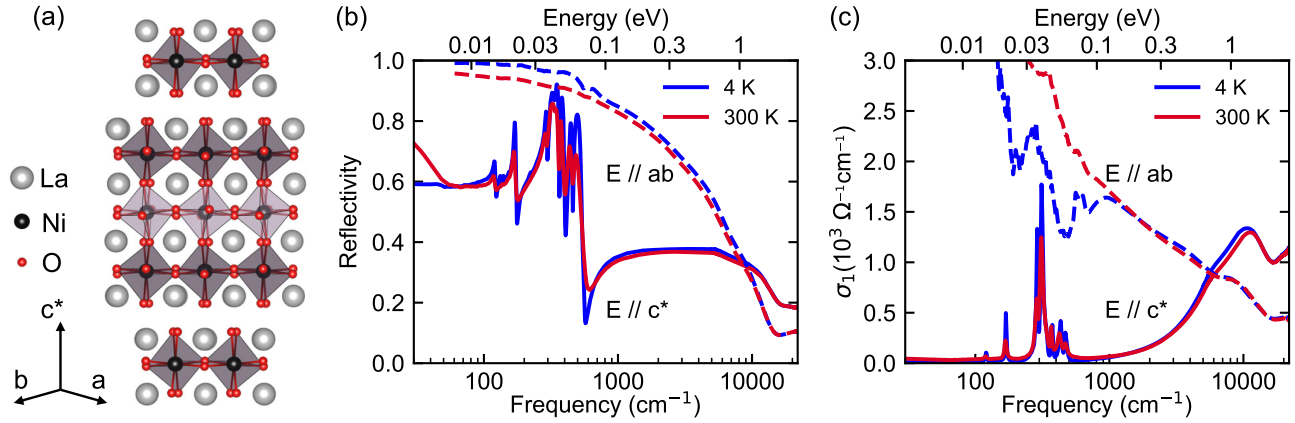

FIG. 1. (a) Structure of the trilayer Ruddlesden-Popper nickelate $La_4Ni_3O_{10}$, consisting of three NiO_3 octahedral layers, where the inner and outer layers are colored differently to reflect their distinct local electronic environments. (b) Reflectivity and (c) real part of the optical conductivity σ_1 at base (blue) and room temperature (red). Out-of-plane ($E\|c^*$) and in-plane ($E\|ab$) optical responses are shown in solid lines and broken lines, respectively. The DW transition temperature is approximately 140 K.

structure. The optical response of this trilayer nickelate is strongly anisotropic. The in-plane reflectivity is metallic, exceeding 0.9 below 500 cm^{-1} and exhibiting a clear plasma edge around 10 000 cm^{-1}. In contrast, the out-of-plane reflectivity is nearly insulating, with only a minor conductivity contribution (likely from hopping conduction) and several infrared-active phonons. This qualitative dichotomy mirrors layered cuprates, where metallic CuO_2 planes coexist with a nearly insulating interlayer response [44]. Figure 1(c) shows the optical conductivity from Kramers-Kronig transformations [45,46] (see SM, Sec. S1 [27]). The optical absorption reveals that the large electronic anisotropy surprisingly reverses around 5000 cm^{-1}. At low frequencies, the in-plane conductivity dominates, consistent with quasi-two-dimensional metallicity, whereas at higher energies, the out-of-plane conductivity exceeds the in-plane component. This crossover signals a clear energy-scale separation of orbital excitations. The high-energy response is set by strong out-of-plane coupling mediated by Ni d_{z^2} orbitals, while the low-energy electrodynamics is dominated by in-plane Ni $d_{x^2-y^2}$, with a substantially reduced d_{z^2} contribution [21].

The observed frequency-dependent reversal in the optical anisotropy is unusual among layered correlated materials. In cuprate superconductors, the infrared optical response is dominated by in-plane $d_{x^2-y^2}$ orbitals, while the out-of-plane conductivity is suppressed by roughly an order of magnitude across the entire infrared range without signs of anisotropy reversals [44,47–50]. In iron-based superconductors, despite their multiorbital and more three-dimensional electronic structure, the in-plane conductivity still exceeds the out-of-plane response, with anisotropy ratios typically ranging between 1 and 10 and, again, no reported reversal [51–54]. The anisotropy reversal of our trilayer nickelate thus reflects a marked multiorbital nature, where distinct orbitals dominate the electronic properties at different energy scales, akin to earlier reports on $La_{2-x}Sr_xNiO_4$ and theoretical predictions for $La_3Ni_2O_7$ [55,56].

Below the DW transition, the in-plane optical conductivity remains metallic but shows a partial mid-infrared depletion of spectral weight associated with the opening of a DW gap [Fig. 1(c)]. We extract the DW gap by analyzing the differential optical conductivity (see SM, Sec. S3 [27]). At base temperature, we obtain an energy gap $2\Delta_{\mathrm{DW}} = 112$ meV, corresponding to $2\Delta_{\mathrm{DW}}/k_B T_{\mathrm{DW}} \approx 9.3$. This ratio is well above the weak-coupling value of 3.52, yet comparable to that of $La_3Ni_2O_7$ [57] and consistent with earlier estimates for $La_4Ni_3O_{10}$ [16,58–60]. A full temperature dependence, shown in SM Fig. S1 [27], verifies that this change occurs continuously. The gap $\Delta(T)$ follows a mean-field behavior, in line with prior x-ray diffraction and neutron scattering [13], and points to a second-order transition, likely driven by an SDW instability [61].

Figures 2(a)–2(d) show the main result of our Letter, where we observe a dramatic effect of the density wave on the temperature dependence of the low-frequency in- and out-of-plane optical conductivity. At frequencies below the phonon and interband contributions, we simultaneously fit the real and imaginary optical conductivity with a simplified Drude + ε_∞ model and obtain extrapolated DC resistivities ρ_{ab} and ρ_{c^*} from $\rho_{\mathrm{dc}} = \lim_{\omega\to 0} 1/\sigma_1(\omega)$ at each temperature [Fig. 2(e)]. While ρ_{ab} remains metallic across the entire temperature range, showing only a weak kink at T_{DW}, ρ_{c^*} rises abruptly by nearly a factor of 5 upon cooling through T_{DW}. As a result, the anisotropy ratio ρ_{c^*}/ρ_{ab} [Fig. 2(f), inset] grows by over an order of magnitude, from $\rho_{c^*}/\rho_{ab} \simeq 70$ at room temperature to $\rho_{c^*}/\rho_{ab} \simeq 2600$ at 4 K, with the sharpest enhancement occurring at the DW transition. We also note that these optically extrapolated DC resistivities agree with separately measured DC transport measurement results [shown as broken lines in Fig. 2(e)]. These results show that the DW transition drives a strongly anisotropic reorganization of charge dynamics, with out-of-plane

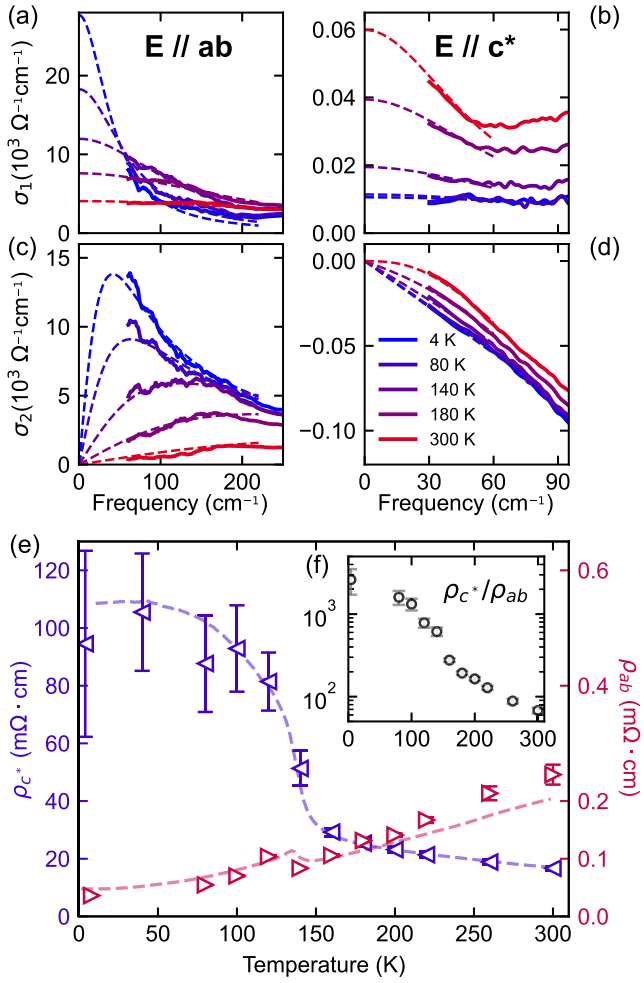

FIG. 2. (a)–(d) Temperature-dependent real and imaginary optical conductivity of $La_4Ni_3O_{10}$ in- ($E\|ab$) and out-of-plane ($E\|c^*$), denoted as solid lines. Drude + ε_∞ model fits are shown as dashed lines. (e) Temperature dependence of the extrapolated DC resistivity obtained from the Drude fits. Left- and right-pointing triangles with error bars represent the out-of-plane (ρ_{c^*}) and in-plane (ρ_{ab}) resistivities, respectively. Broken lines denote DC resistivity obtained from transport measurements. ρ_{ab} is adapted from Ref. [62] (see SM, Sec. S6 [27] for further details). (f) Inset: temperature-dependent resistivity anisotropy ratio ρ_{c^*}/ρ_{ab}.

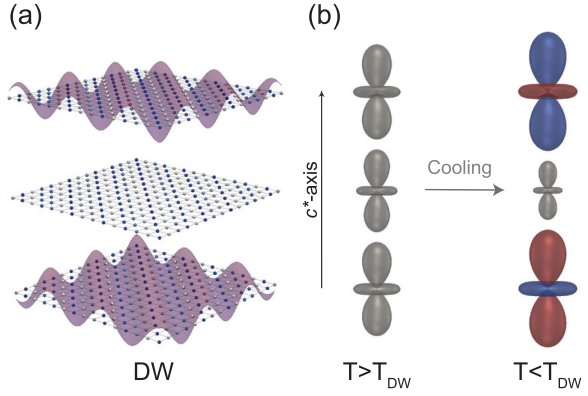

FIG. 3. (a) Real-space depiction of the DW modulation. Below T_{DW}, an antiphase SDW develops on the outer layers, leaving the inner layer as a magnetic node, while the intertwined CDW is in phase across the trilayer. The SDW is indicated by the purple wave and the CDW by the blue-white variation in the lattice color. (b) Possible DW-driven redistribution of Ni d_{z^2} orbital occupation within a trilayer. Above T_{DW}, the trilayer is nonmagnetic, and the d_{z^2} occupation is comparable in inner and outer Ni-O layers despite their inequivalent local environments. Below T_{DW}, the SDW residing on the outer layers (with a magnetic node on the inner layer) is accompanied by an enhanced d_{z^2} weight on the outer layers and a reduced weight on the inner layer, thereby suppressing interlayer transport. The inverted colors on the outer layer d_{z^2} orbitals illustrate the phase of the SDW modulation.

transport suppressed far more than that of in-plane. The large and strongly temperature-dependent anisotropy is consistent with an effective dimensional crossover, meaning that the electronic properties transition from a moderately three-dimensional character at high temperature to a highly two-dimensional character in the low-temperature DW phase.

We argue that the enhanced electronic anisotropy follows from an effective decoupling of the layers within each trilayer subunit (Fig. 3). In trilayer RP nickelates, strong interlayer hybridization of the Ni d_{z^2} orbitals produces three molecular sub-bands (bonding, nonbonding, antibonding) quantum confined by La-O spacer layers between successive Ni-O trilayers. The bonding and antibonding states carry d_{z^2} weight on all three layers, whereas the odd-symmetry nonbonding band has a node on the inner Ni layer. As a result, layer-differentiated filling of the d_{z^2} orbitals emerges naturally in this system, independent of temperature [21,22,25,63,64]. Upon cooling into the DW state, diffraction has established that $La_4Ni_3O_{10}$ develops an intertwined SDW-CDW state in which the SDW resides on the two outer Ni-O layers, leaving the inner layer as a magnetically strongly suppressed node [13,26] [Fig. 3(a)]. A natural interpretation of the effective layer decoupling is that DW order reconstructs the d_{z^2}-derived trilayer states that govern out-of-plane transport. Although optics cannot uniquely determine the underlying microscopic mechanism, it establishes a strong suppression of the d_{z^2} mediated interlayer response in the DW phase, consistent with our calculations showing a reduced interlayer d_{z^2} hopping (see SM, Sec. S10 [27]). One possible route, implied by theory [21,65], is a redistribution of d_{z^2} weight that promotes the nonbonding component. Such a component is concentrated on the outer Ni sites and has negligible inner-layer weight, thus increasing d_{z^2} occupation on the outer layers while lowering it on the inner layer [Fig. 3(b)]. This scenario would reduce the effective interlayer overlap of the d_{z^2} orbitals and suppress the out-of-plane transport. Alternatively, the DW state could also suppress the low-energy c^*-axis response through a partial gap opening on d_{z^2}-derived states [66], loss of quasiparticle coherence [67], or form-factor effects [68].

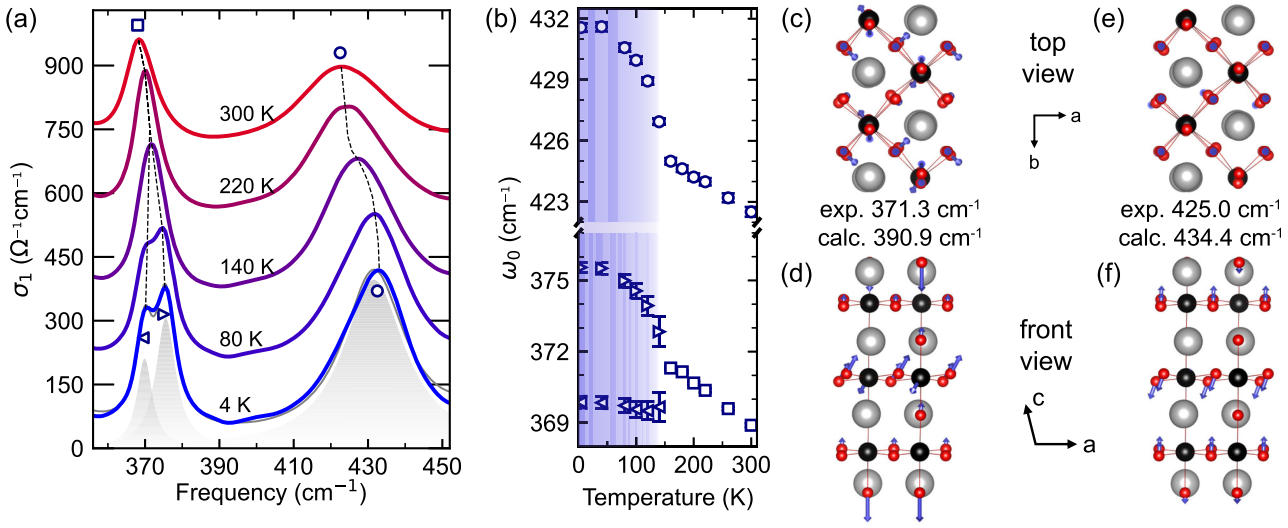

FIG. 4. (a) Temperature evolution of the out-of-plane vibrational response. Spectra are vertically offset by 150 Ω^{-1} cm^{-1} for clarity. Symbols mark phonon frequencies, and dotted lines are guides to the eye. Drude-Lorentz fits to the 4 K spectrum with individual contributions are shown as gray lines and shaded areas, respectively. (b) Temperature-dependent phonon frequencies for selected modes; triangles denote split modes in the DW phase (blue shading). (c)–(f) Calculated atomic displacements for infrared-active modes matching the 160 K data in panel (b); only large-amplitude displacements are shown for clarity. Owing to the monoclinic angle β, the crystallographic c axis is tilted by $\sim$11° relative to the experimental out-of-plane c^* direction. (c), (d) and (e), (f) are views of the same mode from two different directions.

This electronic layer decoupling is supported by the kinetic-energy renormalization $K_{\mathrm{exp}}/K_{\mathrm{DFT}}$ (SM, Sec. S4 [27]), where K_{exp} is obtained from the Drude plasma frequency and K_{DFT} from uncorrelated DFT. At 160 K (above T_{DW}), we find $K^{ab}_{\mathrm{exp}}/K^{ab}_{\mathrm{DFT}} = 0.237$, consistent with a moderately correlated metal [58,69], while the c^*-axis renormalization is far stronger, $K^{c^*}_{\mathrm{exp}}/K^{c^*}_{\mathrm{DFT}} = 0.032$. The resulting anisotropy implies that c^*-axis charge dynamics, set by d_{z^2}-mediated interlayer hopping, is already strongly correlated at high temperature, and thus, is especially susceptible to the DW transition, consistent with the observed layer decoupling.

The pronounced enhancement of the low-energy electronic anisotropy highlights the distinctive place of RP nickelates within the landscape of unconventional superconductors. Cuprates typically display very large, strongly temperature-dependent electronic anisotropy, sometimes accompanied by signatures of a dimensional crossover toward a highly two-dimensional low-energy state [70–77]. However, their physics is effectively described by a single $d_{x^2-y^2}$ orbital. By contrast, iron-based superconductors, where multiple orbitals contribute comparably to both in-plane and out-of-plane transport, exhibit only moderate anisotropy with weak temperature dependence [53,78–85]. Our data show that $La_4Ni_3O_{10}$ realizes an intermediate regime where several orbitals remain active near E_F and interlayer coupling is appreciable. Yet once DW order sets in, it sharply amplifies the transport anisotropy by effectively decoupling the Ni-O layers within each trilayer subunit, enhancing the two-dimensional character of the low-energy charge dynamics [8,86].

Beyond reshaping the low-energy electrodynamics, the DW transition also imprints clear signatures in the c^*-axis vibrational spectrum. Analysis of the infrared-active phonons (see SM, Sec. S9 [27]) shows that the strongest effects occur between 350 and 450 cm^{-1} [Figs. 4(a) and 4(b)]. Upon cooling into the DW state, the 370 cm^{-1} peak splits into two branches, while the 430 cm^{-1} peak strongly hardens without splitting [Fig. 4(b)]. Additionally, weaker anomalies are discussed in the SM, Sec. S9 [27], but in all cases, the low-temperature evolution departs significantly from the smooth anharmonic trends above T_{DW}. We compared the room-temperature results to first-principles calculations for the monoclinic $P2_1/a$ crystal symmetry. Based on this analysis, we associate the phonons at 371 and 425 cm^{-1} to the calculated eigenvectors in Figs. 4(c)–4(f). These are dominated by Ni-O bond distortions with mixed bending and stretching, implying that the DW primarily perturbs lattice distortions coupled to charge modulation in the Ni-O layers.

These vibrational anomalies could originate from (i) a structural transition, (ii) zone folding by the DW superlattice, (iii) electron-phonon coupling, or (iv) magnetoelastic coupling. Across the DW transition, diffraction establishes an incommensurate DW lattice modulation (weak satellite reflections with typical intensities $\sim 10^{-4}$ of the fundamental Bragg peaks [13]) while the average structure defined by fundamental reflections shows no resolved space-group change, and the reported lattice-parameter anomalies are

well below the 0.1% level [62,87–89]. Nonetheless, we observe ∼1% frequency shifts and splittings only for certain phonons in a frequency window of 300–500 cm^{-1}, far exceeding expectations from such small structural changes. This mismatch, together with the absence of any resolved average space group change, disfavors an explanation based on a simple lattice instability.

Zone folding by the DW superlattice, which backfolds finite-momentum phonons to the zone center [90], is, in principle, expected in $La_4Ni_3O_{10}$. The CDW exhibits an in-plane superlattice modulation on all Ni-O layers, and its out-of-phase stacking between neighboring trilayers further enlarges the effective periodicity along the out-of-plane direction [13]. This enlarged DW-modulated periodicity can, in principle, activate additional infrared-active phonons. However, zone folding alone does not adequately account for our data. For an incommensurate DW, even the closest five-unit-cell approximant would generically activate many additional modes across the entire vibrational spectrum, thus introducing a much broader distribution of extra features than that observed. Instead, the DW anomalies remain sharp and highly selective, appearing only in a small subset of Ni-O vibrations. Electron-phonon coupling in the DW state is, therefore, a more compelling ingredient. The unidirectional CDW creates an anisotropic charge distribution [13], thereby selectively differentiating previously equivalent local environments and anisotropically renormalizing lattice force constants, which can, in turn, account for the phonon anomaly observed experimentally as a splitting in selected Ni-O peaks. DW-CDW collective modes (amplitude-phase fluctuations) may also couple to infrared phonons and contribute to the observed anomalies [91]. Finally, magnetoelastic coupling may contribute by renormalizing phonon energies and lifetimes and, in some cases, producing mode splitting [92]. Because the CDW in $La_4Ni_3O_{10}$ is intertwined with SDW order with sizable outer-layer ordered moments [14,21,65], and the phonon anomalies occur at energies comparable to magnetic excitations (up to ∼50 meV) reported by resonant inelastic x-ray scattering [93,94], coupling between lattice vibrations and collective spin excitations is a realistic possibility.

In the aggregate, our observations establish $La_4Ni_3O_{10}$ as a strongly anisotropic, multiorbital metal. Upon entering the DW state, its low-energy anisotropy increases by over an order of magnitude, consistent with an effective decoupling of the Ni-O layers within each trilayer subunit. The simplest reading of the optical data is that this process is electronically driven, arising from a DW-induced redistribution of Ni d_{z^2} occupation that quenches interlayer charge dynamics without a resolved change in the average crystallographic space group. While the Ni $d_{x^2-y^2}$ and d_{z^2} orbitals are energetically distinct, with $d_{x^2-y^2}$ states dominating the in-plane metallic state, we find that d_{z^2} orbitals govern both the interband transition and hopping conduction along the out-of-plane direction. Overall, the unique interplay between the two orbitals in layered nickelates defines the low-energy electrodynamics and yields an emergent quasi-two-dimensional response promoted by DW order. The significant impact of the DW state on the lattice dynamics, in the absence of correspondingly large structural changes, further supports a picture in which the DW state is primarily electronic in origin. Our results imply that any microscopic discussion of the superconducting instability in this family should explicitly account for multiorbital effects and changes of the coupling among the layers, providing a concrete point of comparison to cuprates and iron-based superconductors.

Note added—We have become aware of a recent optical study of trilayer $La_4Ni_3O_{10}$ [95]. While the overall phenomenology is consistent, our Letter focuses on the effect of the DW transition on the in- and out-of-plane electronic response below 100–150 cm^{-1} and the vibrational properties, thereby providing complementary information on the low-energy physics of this material.

Acknowledgments—We thank D. Nicoletti, J. Li, S. Priya, and X. Guo for insightful discussions. Work by Z. G., S. F. R. T., M. T., F. G., C. C. H., M. P. M. D., and M. M. was supported by the U.S. Department of Energy (DOE), Office of Science, Division of Basic Energy Science, under Contract No. DE-SC0012704. Part of the experimental work was performed in the Infrared Lab at the National Synchrotron Light Source II, a DOE Office of Science User Facility operated for the DOE Office of Science by Brookhaven National Laboratory. S. F. R. T. acknowledges additional support from the DOE, Office of Science, Office of Workforce Development for Teachers and Scientists, Office of Science Graduate Student Research (SCGSR) program. The SCGSR program is administered by the Oak Ridge Institute for Science and Education for the DOE under Contract No. DE-SC0014664. A. S. B. and Y. Z. acknowledge support from NSF Grant No. DMR-2323971 and the ASU research computing center for HPC resources. Work by X. C. and J. F. M. in the Materials Science Division at Argonne National Laboratory (crystal growth) was supported by the U.S. Department of Energy Office of Science, Basic Energy Sciences, Materials Science and Engineering Division. Work by X. C. and P. K. was supported by AFOSR (FA9550-25-1-0019). A. M. Y. was supported by NSF (DMR-2105048).

Data availability—The data that support the findings of this article are openly available [96].

[1] Hualei Sun, Mengwu Huo, Xunwu Hu, Jingyuan Li, Zengjia Liu, Yifeng Han, Lingyun Tang, Zhongquan Mao, Pengtao Yang, Bosen Wang, Jinguang Cheng, Dao-Xin Yao, Guang-Ming Zhang, and Meng Wang, Signatures

of superconductivity near 80 K in a nickelate under high pressure, Nature (London) **621**, 493 (2023).

[2] Yanan Zhang, Dajun Su, Yanen Huang, Zhaoyang Shan, Hualei Sun, Mengwu Huo, Kaixin Ye, Jiawen Zhang, Zihan Yang, Yongkang Xu, Yi Su, Rui Li, Michael Smidman, Meng Wang, Lin Jiao, and Huiqiu Yuan, High-temperature superconductivity with zero resistance and strange-metal behaviour in $La_3Ni_2O_{7-\delta}$, Nat. Phys. **20**, 1269 (2024).

[3] Yinghao Zhu, Di Peng, Enkang Zhang, Bingying Pan, Xu Chen, Lixing Chen, Huifen Ren, Feiyang Liu, Yiqing Hao, Nana Li *et al.*, Superconductivity in pressurized trilayer $La_4Ni_3O_{10-\delta}$ single crystals, Nature (London) **631**, 531 (2024).

[4] Meng Wang, Hai-Hu Wen, Tao Wu, Dao-Xin Yao, and Tao Xiang, Normal and superconducting properties of $La_3Ni_2O_7$, Chin. Phys. Lett. **41**, 077402 (2024).

[5] Hirofumi Sakakibara, Masayuki Ochi, Hibiki Nagata, Yuta Ueki, Hiroya Sakurai, Ryo Matsumoto, Kensei Terashima, Keisuke Hirose, Hiroto Ohta, Masaki Kato, Yoshihiko Takano, and Kazuhiko Kuroki, Theoretical analysis on the possibility of superconductivity in the trilayer Ruddlesden–Popper nickelate $La_4Ni_3O_{10}$ under pressure and its experimental examination: comparison with $La_3Ni_2O_7$, Phys. Rev. B **109**, 144511 (2024).

[6] Mingxin Zhang, Cuiying Pei, Di Peng, Xian Du, Weixiong Hu, Yantao Cao, Qi Wang, Juefei Wu, Yidian Li, Huanyu Liu *et al.*, Superconductivity in trilayer nickelate $La_4Ni_3O_{10}$ under pressure, Phys. Rev. X **15**, 021005 (2025).

[7] Qing Li, Ying-Jie Zhang, Zhe-Ning Xiang, Yuhang Zhang, Xiyu Zhu, and Hai-Hu Wen, Signature of superconductivity in pressurized $La_4Ni_3O_{10}$, Chin. Phys. Lett. **41**, 017401 (2024).

[8] Pascal Puphal, Thomas Schäfer, Bernhard Keimer, and Matthias Hepting, Superconductivity in infinite-layer and Ruddlesden-Popper nickelates, Nat. Rev. Phys. **8**, 70 (2026).

[9] Yuxin Wang, Kun Jiang, Jianjun Ying, Tao Wu, Jinguang Cheng, Jiangping Hu, and Xianhui Chen, Recent progress in nickelate superconductors, Natl. Sci. Rev. **12**, nwaf373 (2025).

[10] Kaiwen Chen, Xiangqi Liu, Jiachen Jiao, Muyuan Zou, Chengyu Jiang, Xin Li, Yixuan Luo, Qiong Wu, Ningyuan Zhang, Yanfeng Guo, and Lei Shu, Evidence of spin density waves in $La_3Ni_2O_{7-\delta}$, Phys. Rev. Lett. **132**, 256503 (2024).

[11] Tao Xie, Mengwu Huo, Xiaosheng Ni, Feiran Shen, Xing Huang, Hualei Sun, Helen C. Walker, Devashibhai Adroja, Dehong Yu, Bing Shen, Lunhua He, Kun Cao, and Meng Wang, Strong interlayer magnetic exchange coupling in $La_3Ni_2O_{7-\delta}$ revealed by inelastic neutron scattering, Sci. Bull. **69**, 3221 (2024).

[12] Rustem Khasanov, Thomas J. Hicken, Dariusz J. Gawryluk, Vahid Sazgari, Igor Plokhikh, Loïc Pierre Sorel, Marek Bartkowiak, Steffen Bötzel, Frank Lechermann, Ilya M. Eremin, Hubertus Luetkens, and Zurab Guguchia, Pressure-enhanced splitting of density wave transitions in $La_3Ni_2O_{7-\delta}$, Nat. Phys. **21**, 430 (2025).

[13] Junjie Zhang, D. Phelan, A. S. Botana, Yu-Sheng Chen, Hong Zheng, M. Krogstad, Suyin Grass Wang, Yiming Qiu, J. A. Rodriguez-Rivera, R. Osborn, S. Rosenkranz, M. R. Norman, and J. F. Mitchell, Intertwined density waves in a metallic nickelate, Nat. Commun. **11**, 6003 (2020).

[14] Rustem Khasanov, Vahid Sazgari, Thomas J. Hicken, Igor Plokhikh, Marisa Medarde, Ekaterina Pomjakushina, Lukas Keller, Vladimir Pomjakushin, Marek Bartkowiak, Szymon Królak, Michal J. Winiarski, Alexander Steppke, Jonas A. Krieger, Hubertus Luetkens, Tomasz Klimczuk, Christof W. Schneider, Dariusz J. Gawryluk, and Zurab Guguchia, Pressure and oxygen-isotope substitution on density-wave transitions in $La_4Ni_3O_{10}$, Phys. Rev. Res. **8**, 013249 (2026).

[15] Shuxiang Xu, Hao Wang, Mengwu Huo, Deyuan Hu, Qiong Wu, Li Yue, Dong Wu, Meng Wang, Tao Dong, and Nanlin Wang, Collapse of density wave and emergence of superconductivity in pressurized $La_4Ni_3O_{10}$ evidenced by ultrafast spectroscopy, Nat. Commun. **16**, 7039 (2025).

[16] Dong-Hyeon Gim, Chung Ha Park, and Kee Hoon Kim, Orbital-selective quasiparticle depletion across the density wave transition in trilayer nickelate $La_4Ni_3O_{10}$, Phys. Rev. Lett. **135**, 136505 (2025).

[17] Ming Zhang, Hongyi Sun, Yu-Bo Liu, Qihang Liu, Wei-Qiang Chen, and Fan Yang, Spin-density wave and superconductivity in $La_4Ni_3O_{10}$ under ambient pressure, Phys. Rev. B **111**, 144502 (2025).

[18] Cui-Qun Chen, Zhihui Luo, Meng Wang, Wéi Wú, and Dao-Xin Yao, Trilayer multiorbital models of $La_4Ni_3O_{10}$, Phys. Rev. B **110**, 014503 (2024).

[19] Qing-Geng Yang, Kai-Yue Jiang, Da Wang, Hong-Yan Lu, and Qiang-Hua Wang, Effective model and $s_\pm$-wave superconductivity in trilayer nickelate $La_4Ni_3O_{10}$, Phys. Rev. B **109**, L220506 (2024).

[20] Yang Zhang, Ling-Fang Lin, Adriana Moreo, Thomas A. Maier, and Elbio Dagotto, Prediction of $s_\pm$-wave superconductivity enhanced by electronic doping in trilayer nickelates $La_4Ni_3O_{10}$ under pressure, Phys. Rev. Lett. **133**, 136001 (2024).

[21] Harrison LaBollita, Jesse Kapeghian, Michael R. Norman, and Antia S. Botana, Electronic structure and magnetic tendencies of trilayer $La_4Ni_3O_{10}$ under pressure: Structural transition, molecular orbitals, and layer differentiation, Phys. Rev. B **109**, 195151 (2024).

[22] I. V. Leonov, Electronic structure and magnetic correlations in the trilayer nickelate superconductor $La_4Ni_3O_{10}$ under pressure, Phys. Rev. B **109**, 235123 (2024).

[23] Peng-Fei Tian, Hao-Tian Ma, Xing Ming, Xiao-Jun Zheng, and Huan Li, Effective model and electron correlations in trilayer nickelate superconductor $La_4Ni_3O_{10}$, J. Phys. Condens. Matter **36**, 355602 (2024).

[24] Junkang Huang and Tao Zhou, Interlayer pairing-induced partially gapped Fermi surface in trilayer $La_4Ni_3O_{10}$ superconductors, Phys. Rev. B **110**, L060506 (2024).

[25] Jing-Xuan Wang, Zhenfeng Ouyang, Rong-Qiang He, and Zhong-Yi Lu, Non-Fermi liquid and Hund correlation in $La_4Ni_3O_{10}$ under high pressure, Phys. Rev. B **109**, 165140 (2024).

[26] Anjana M. Samarakoon, J. Strempfer, Junjie Zhang, Feng Ye, Yiming Qiu, J.-W. Kim, H. Zheng, S. Rosenkranz, M. R. Norman, J. F. Mitchell, and D. Phelan, Bootstrapped dimensional crossover of a spin density wave, Phys. Rev. X **13**, 041018 (2023).

[27] See Supplemental Material at http://link.aps.org/supplemental/10.1103/qgl1-zh9f for details on sample preparation, optical measurements, Drude-Lorentz analysis and DFT calculations of the optical response, extraction of the density wave gap, electronic correlation calculation, transport resistivity measurements, and analysis of phonon modes, which also includes Refs. [28–43].

[28] Christopher C. Homes, M. Reedyk, D. A. Cradles, and T. Timusk, Technique for measuring the reflectance of irregular, submillimeter-sized samples, Appl. Opt. **32**, 2976 (1993).

[29] C. C. Homes, J. M. Tranquada, and D. J. Buttrey, Stripe order and vibrational properties of $La_2NiO_{4+\delta}$ for $\delta = 2/15$: measurements and *ab initio* calculations, Phys. Rev. B **75**, 045128 (2007).

[30] Hari Padma, Filippo Glerean, Sophia F. R. TenHuisen, Zecheng Shen, Haoxin Wang, Luogen Xu, Joshua D. Elliott, Christopher C. Homes, Elizabeth Skoropata, Hiroki Ueda *et al.*, Symmetry-protected electronic metastability in an optically driven cuprate ladder, Nat. Mater. **24**, 1584 (2025).

[31] Frank Y. Gao, Zhuquan Zhang, Zi-Jie Liu, and Keith A. Nelson, High-speed two-dimensional terahertz spectroscopy with echelon-based shot-to-shot balanced detection, Opt. Lett. **47**, 3479 (2022).

[32] Peter Blaha, Karlheinz Schwarz, Fabien Tran, Robert Laskowski, Georg K. H. Madsen, and Laurence D. Marks, WIEN2k: An APW + LO program for calculating the properties of solids, J. Chem. Phys. **152**, 074101 (2020).

[33] John P. Perdew, Kieron Burke, and Matthias Ernzerhof, Generalized gradient approximation made simple, Phys. Rev. Lett. **77**, 3865 (1996).

[34] A. Seidl, A. Görling, P. Vogl, J. A. Majewski, and M. Levy, Generalized Kohn-Sham schemes and the band-gap problem, Phys. Rev. B **53**, 3764 (1996).

[35] M. M. Qazilbash, J. J. Hamlin, R. E. Baumbach, Lijun Zhang, D. J. Singh, M. B. Maple, and D. N. Basov, Electronic correlations in the iron pnictides, Nat. Phys. **5**, 647 (2009).

[36] Leonardo Degiorgi, Electronic correlations in iron-pnictide superconductors and beyond: lessons learned from optics, New J. Phys. **13**, 023011 (2011).

[37] Shangxiong Huangfu, Gawryluk Dariusz Jakub, Xiaofu Zhang, Olivier Blacque, Pascal Puphal, Ekaterina Pomjakushina, Fabian O. von Rohr, and Andreas Schilling, Anisotropic character of the metal-to-metal transition in $Pr_4Ni_3O_{10}$, Phys. Rev. B **101**, 104104 (2020).

[38] Atsushi Togo and Isao Tanaka, First principles phonon calculations in materials science, Scr. Mater. **108**, 1 (2015).

[39] R. Boehler and J. Ramakrishnan, Experimental results on the pressure dependence of the Grüneisen parameter: A review, J. Geophys. Res. **85**, 6996 (1980).

[40] R. J. Bruls, H. T. Hintzen, G. de With, R. Metselaar, and J. C. van Miltenburg, The temperature dependence of the Grüneisen parameters of $MgSiN_2$, AlN and β-Si_3N_4, J. Phys. Chem. Solids **62**, 783 (2001).

[41] M. Balkanski, R. F. Wallis, and E. Haro, Anharmonic effects in light scattering due to optical phonons in silicon, Phys. Rev. B **28**, 1928 (1983).

[42] Giovanni Pizzi, Valerio Vitale, Ryotaro Arita, Stefan Blügel, Frank Freimuth, Guillaume Géranton, Marco Gibertini, Dominik Gresch, Charles Johnson, Takashi Koretsune *et al.*, Wannier90 as a community code: New features and applications, J. Phys. Condens. Matter **32**, 165902 (2020).

[43] S. L. Dudarev, G. A. Botton, S. Y. Savrasov, C. J. Humphreys, and A. P. Sutton, Electron-energy-loss spectra and the structural stability of nickel oxide: An LSDA + U study, Phys. Rev. B **57**, 1505 (1998).

[44] D. N. Basov and T. Timusk, Electrodynamics of high-T_c superconductors, Rev. Mod. Phys. **77**, 721 (2005).

[45] Martin Dressel and George Grüner, *Electrodynamics of Solids: Optical Properties of Electrons in Matter* (Cambridge University Press, Cambridge, England, 2002).

[46] D. B. Tanner, Use of x-ray scattering functions in Kramers-Kronig analysis of reflectance, Phys. Rev. B **91**, 035123 (2015).

[47] S. Uchida, K. Tamasaku, and S. Tajima, *c*-axis optical spectra and charge dynamics in $La_{2-x}Sr_xCuO_4$, Phys. Rev. B **53**, 14558 (1996).

[48] C. C. Homes, T. Timusk, D. A. Bonn, R. Liang, and W. N. Hardy, Optical properties along the *c*-axis of $YBa_2Cu_3O_{6+x}$, for $x = 0.50$–0.95: Evolution of the pseudogap, Physica (Amsterdam) **254C**, 265 (1995).

[49] S. L. Cooper, D. Reznik, A. Kotz, M. A. Karlow, R. Liu, M. V. Klein, W. C. Lee, J. Giapintzakis, D. M. Ginsberg, B. W. Veal, and A. P. Paulikas, Optical studies of the *a*-, *b*-, and *c*-axis charge dynamics in $YBa_2Cu_3O_{6+x}$, Phys. Rev. B **47**, 8233 (1993).

[50] J. Schützmann, S. Tajima, S. Miyamoto, and S. Tanaka, *c*-axis optical response of fully oxygenated $YBa_2Cu_3O_{7-\delta}$: Observation of dirty-limit-like superconductivity and residual unpaired carriers, Phys. Rev. Lett. **73**, 174 (1994).

[51] Z. G. Chen, T. Dong, R. H. Ruan, B. F. Hu, B. Cheng, W. Z. Hu, P. Zheng, Z. Fang, X. Dai, and N. L. Wang, Measurement of the *c*-axis optical reflectance of AFe_2As_2 ($A = \mathrm{Ba, Sr}$) single crystals: Evidence of different mechanisms for the formation of two energy gaps, Phys. Rev. Lett. **105**, 097003 (2010).

[52] B. Cheng, Z. G. Chen, C. L. Zhang, R. H. Ruan, T. Dong, B. F. Hu, W. T. Guo, S. S. Miao, P. Zheng, J. L. Luo, G. Xu, P. Dai, and N. L. Wang, Three-dimensionality of band structure and a large residual quasiparticle population in $Ba_{0.67}K_{0.33}Fe_2As_2$ as revealed by *c*-axis polarized optical measurements, Phys. Rev. B **83**, 144522 (2011).

[53] S. J. Moon, C. C. Homes, A. Akrap, Z. J. Xu, J. S. Wen, Z. W. Lin, Q. Li, G. D. Gu, and D. N. Basov, Incoherent *c*-axis interplane response of the iron chalcogenide $FeTe_{0.55}Se_{0.45}$ superconductor from infrared spectroscopy, Phys. Rev. Lett. **106**, 217001 (2011).

[54] S. J. Moon, A. A. Schafgans, M. A. Tanatar, R. Prozorov, A. Thaler, P. C. Canfield, A. S. Sefat, D. Mandrus, and D. N. Basov, Interlayer coherence and superconducting condensate in the *c*-axis response of optimally doped $Ba(Fe_{1-x}Co_x)_2As_2$ high-T_c superconductor using infrared spectroscopy, Phys. Rev. Lett. **110**, 097003 (2013).

[55] S. Shinomori, M. Kawasaki, and Y. Tokura, Orientation-controlled epitaxy and anisotropic properties of

$La_{2-x}Sr_xNiO_4$ with $0.5 \leq x \leq 1.5$ covering the insulator–metal transition, Appl. Phys. Lett. **80**, 574 (2002).

[56] Benjamin Geisler, Laura Fanfarillo, James J. Hamlin, Gregory R. Stewart, Richard G. Hennig, and P. J. Hirschfeld, Optical properties and electronic correlations in $La_3Ni_2O_7$ bilayer nickelates under high pressure, npj Quantum Mater. **9**, 89 (2024).

[57] Zhe Liu, Mengwu Huo, Jie Li, Qing Li, Yuecong Liu, Yaomin Dai, Xiaoxiang Zhou, Jiahao Hao, Yi Lu, Meng Wang, and Hai-Hu Wen, Electronic correlations and partial gap in the bilayer nickelate $La_3Ni_2O_7$, Nat. Commun. **15**, 7570 (2024).

[58] Shuxiang Xu, Cui-Qun Chen, Mengwu Huo, Deyuan Hu, Hao Wang, Qiong Wu, Rongsheng Li, Dong Wu, Meng Wang, Dao-Xin Yao, Tao Dong, and Nanlin Wang, Origin of the density wave instability in trilayer nickelate $La_4Ni_3O_{10}$ revealed by optical and ultrafast spectroscopy, Phys. Rev. B **111**, 075140 (2025).

[59] Mingzhe Li, Jiashuo Gong, Yinghao Zhu, Ziyuan Chen, Jiakang Zhang, Enkang Zhang, Yuanji Li, Ruotong Yin, Shiyuan Wang, Jun Zhao, Dong-Lai Feng, Zengyi Du, and Ya-Jun Yan, Direct visualization of an incommensurate unidirectional charge density wave in $La_4Ni_3O_{10}$, Phys. Rev. B **112**, 045132 (2025).

[60] A. Suthar, V. Sundaramurthy, M. Bejas, Congcong Le, P. Puphal, P. Sosa-Lizama, A. Schulz, J. Nuss, M. Isobe, P. A. van Aken, Y. E. Suyolcu, M. Minola, A. P. Schnyder, X. Wu, B. Keimer, G. Khaliullin, A. Greco, and M. Hepting, Multiorbital character of the density wave instability in $La_4Ni_3O_{10}$, arXiv:2508.06440.

[61] M. R. Norman, Landau theory of the density wave transition in trilayer Ruddlesden-Popper nickelates, Phys. Rev. B **112**, 075149 (2025).

[62] Junjie Zhang, Hong Zheng, Yu-Sheng Chen, Yang Ren, Masao Yonemura, Ashfia Huq, and J. F. Mitchell, High oxygen pressure floating zone growth and crystal structure of the metallic nickelates $R_4Ni_3O_{10}$ ($R = \mathrm{La}, \mathrm{Pr}$), Phys. Rev. Mater. **4**, 083402 (2020).

[63] Victor Pardo and Warren E. Pickett, Quantum confinement induced molecular correlated insulating state in $La_4Ni_3O_8$, Phys. Rev. Lett. **105**, 266402 (2010).

[64] Myung-Chul Jung, Jesse Kapeghian, Chase Hanson, Betül Pamuk, and Antia S. Botana, Electronic structure of higher-order Ruddlesden-Popper nickelates, Phys. Rev. B **105**, 085150 (2022).

[65] Binhua Zhang, Changsong Xu, and Hongjun Xiang, Spin-charge-orbital order in nickelate superconductors, Phys. Rev. B **111**, 184401 (2025).

[66] Haoxiang Li, Xiaoqing Zhou, Thomas Nummy, Junjie Zhang, Victor Pardo, Warren E. Pickett, J. F. Mitchell, and D. S. Dessau, Fermiology and electron dynamics of trilayer nickelate $La_4Ni_3O_{10}$, Nat. Commun. **8**, 704 (2017).

[67] Bo Su, Chaoxin Huang, Jianzhou Zhao, Mengwu Huo, Jianlin Luo, Meng Wang, and Zhi-Guo Chen, Strongly anisotropic charge dynamics in $La_3Ni_2O_7$ with coherent-to-incoherent crossover of interlayer charge dynamics, arXiv:2411.10786.

[68] Kazuhiro Fujita, Mohammad H. Hamidian, Stephen D. Edkins, Chung Koo Kim, Yuhki Kohsaka, Masaki Azuma, Mikio Takano, Hidenori Takagi, Hiroshi Eisaki, Shin-ichi Uchida, Andrea Allais, Michael J. Lawler, Eun-Ah Kim, Subir Sachdev, and J. C. Séamus Davis, Direct phase-sensitive identification of a *d*-form factor density wave in underdoped cuprates, Proc. Natl. Acad. Sci. U.S.A. **111**, E3026 (2014).

[69] Zhe Liu, Jie Li, Mengwu Huo, Bingke Ji, Jiahao Hao, Yaomin Dai, Mengjun Ou, Qing Li, Hualei Sun, Bing Xu, Yi Lu, Meng Wang, and Hai-Hu Wen, Evolution of electronic correlations in the Ruddlesden-Popper nickelates, Phys. Rev. B **111**, L220505 (2025).

[70] Y. Nakamura and S. Uchida, Anisotropic transport properties of single-crystal $La_{2-x}Sr_xCuO_4$: Evidence for the dimensional crossover, Phys. Rev. B **47**, 8369 (1993).

[71] Seiki Komiya, Yoichi Ando, X. F. Sun, and A. N. Lavrov, *c*-axis transport and resistivity anisotropy of lightly to moderately doped $La_{2-x}Sr_xCuO_4$ single crystals: Implications on the charge transport mechanism, Phys. Rev. B **65**, 214535 (2002).

[72] S. Martin, A. T. Fiory, R. M. Fleming, L. F. Schneemeyer, and J. V. Waszczak, Temperature dependence of the resistivity tensor in superconducting $Bi_2Sr_{2.2}Ca_{0.8}Cu_2O_8$ crystals, Phys. Rev. Lett. **60**, 2194 (1988).

[73] T. Watanabe, T. Fujii, and A. Matsuda, Anisotropic resistivities of precisely oxygen controlled single-crystal $Bi_2Sr_2CaCu_2O_{8+\delta}$: Systematic study on "spin gap" effect, Phys. Rev. Lett. **79**, 2113 (1997).

[74] V. N. Zavaritsky and A. S. Alexandrov, Normal state of extremely anisotropic superconducting cuprates as revealed by magnetotransport, Phys. Rev. B **71**, 012502 (2005).

[75] K. Takenaka, K. Mizuhashi, H. Takagi, and S. Uchida, Interplane charge transport in $YBa_2Cu_3O_{7-y}$: Spin-gap effect on in-plane and out-of-plane resistivity, Phys. Rev. B **50**, 6534 (1994).

[76] N. E. Hussey, K. Nozawa, H. Takagi, S. Adachi, and K. Tanabe, Anisotropic resistivity of $YBa_2Cu_4O_8$: Incoherent-to-metallic crossover in the out-of-plane transport, Phys. Rev. B **56**, R11423 (1997).

[77] A. N. Lavrov, M. Yu. Kameneva, and L. P. Kozeeva, Normal-state resistivity anisotropy in underdoped $RBa_2Cu_3O_{6+x}$ crystals, Phys. Rev. Lett. **81**, 5636 (1998).

[78] X. F. Wang, T. Wu, G. Wu, H. Chen, Y. L. Xie, J. J. Ying, Y. J. Yan, R. H. Liu, and X. H. Chen, Anisotropy in the electrical resistivity and susceptibility of superconducting $BaFe_2As_2$ single crystals, Phys. Rev. Lett. **102**, 117005 (2009).

[79] G. F. Chen, Z. Li, J. Dong, G. Li, W. Z. Hu, X. D. Zhang, X. H. Song, P. Zheng, N. L. Wang, and J. L. Luo, Transport and anisotropy in single-crystalline $SrFe_2As_2$ and $A_{0.6}K_{0.4}Fe_2As_2$ ($A = \mathrm{Sr}, \mathrm{Ba}$) superconductors, Phys. Rev. B **78**, 224512 (2008).

[80] M. A. Tanatar, N. Ni, G. D. Samolyuk, S. L. Bud'ko, P. C. Canfield, and R. Prozorov, Resistivity anisotropy of AFe_2As_2 ($A = \mathrm{Ca}, \mathrm{Sr}, \mathrm{Ba}$): Direct versus Montgomery technique measurements, Phys. Rev. B **79**, 134528 (2009).

[81] M. Nakajima, M. Nagafuchi, and S. Tajima, Comprehensive study of out-of-plane transport properties in $BaFe_2As_2$: three-dimensional electronic state and effect of chemical substitution, Phys. Rev. B **97**, 094511 (2018).

[82] Hang-Dong Wang, Chi-Heng Dong, Zu-Juan Li, Qian-Hui Mao, Sha-Sha Zhu, Chun-Mu Feng, H. Q. Yuan, and

Ming-Hu Fang, Superconductivity at 32 K and anisotropy in $Tl_{0.58}Rb_{0.42}Fe_{1.72}Se_2$ crystals, Europhys. Lett. **93**, 47004 (2011).

[83] Hechang Lei and C. Petrovic, Anisotropy in transport and magnetic properties of $K_{0.64}Fe_{1.44}Se_2$, Phys. Rev. B **83**, 184504 (2011).

[84] S. I. Vedeneev, B. A. Piot, D. K. Maude, and A. V. Sadakov, Temperature dependence of the upper critical field of FeSe single crystals, Phys. Rev. B **87**, 134512 (2013).

[85] Yoo Jang Song, Jin Soo Ghim, Byeong Hun Min, Yong Seung Kwon, Myung Hwa Jung, and Jong-Soo Rhyee, Synthesis, anisotropy, and superconducting properties of LiFeAs single crystal, Appl. Phys. Lett. **96**, 212508 (2010).

[86] Zhuoyu Chen and Haoliang Huang, The nickelate bridge between cuprate and iron-based superconductivity, Quantum Front. **4**, 17 (2025).

[87] Susmit Kumar, Øystein Fjellvåg, Anja Olafsen Sjåstad, and Helmer Fjellvåg, Physical properties of Ruddlesden-Popper ($n = 3$) nickelate: $La_4Ni_3O_{10}$, J. Magn. Magn. Mater. **496**, 165915 (2020).

[88] Dibyata Rout, Sanchayeta Ranajit Mudi, Marco Hoffmann, Sven Spachmann, Rüdiger Klingeler, and Surjeet Singh, Structural and physical properties of trilayer nickelates $R_4Ni_3O_{10}$ ($R = \mathrm{La, Pr, Nd}$), Phys. Rev. B **102**, 195144 (2020).

[89] Nana Li, Jiayi Guan, Limin Yan, Xiaozhi Yan, Mingtao Li, Xuqiang Liu, Kai Zhang, Feiyu Li, Shu Cai, Haini Dong, Adama N-Diaye, Monica Amboage, Junjie Zhang, Yantao Cao, Hanjie Guo, Qingyu Kong, Liling Sun, and Wenge Yang, Crystal and electronic structure studies of $La_4Ni_3O_{10-\delta}$ under high-pressure and low-temperature conditions, J. Am. Chem. Soc. **147**, 43717 (2025).

[90] Sonia Deswal, Deepu Kumar, Dibyata Rout, Surjeet Singh, and Pradeep Kumar, Dynamics of electron–electron correlation and electron–phonon coupled phase progression in trilayer nickelate $La_4Ni_3O_{10}$, Appl. Phys. Lett. **127**, 071903 (2025).

[91] George Grüner, The dynamics of charge-density waves, Rev. Mod. Phys. **60**, 1129 (1988).

[92] Dipankar Jana, Diana Vaclavkova, Rajesh Kumar Ulaganathan, Raman Sankar, Milan Orlita, Clement Faugeras, Maciej Koperski, M. E. Zhitomirsky, and Marek Potemski, Strong and selective magnon–phonon coupling in the van der Waals antiferromagnet $CoPS_3$, Phys. Rev. B **112**, 165427 (2025).

[93] Xiaoyang Chen, Jaewon Choi, Zhicheng Jiang, Jiong Mei, Kun Jiang, Jie Li, Stefano Agrestini, Mirian Garcia-Fernandez, Hualei Sun, Xing Huang, Dawei Shen, Meng Wang, Jiangping Hu, Yi Lu, Ke-Jin Zhou, and Donglai Feng, Electronic and magnetic excitations in $La_3Ni_2O_7$, Nat. Commun. **15**, 9597 (2024).

[94] Sophia F. R. TenHuisen, Grace A. Pan, Qi Song, Denitsa R. Baykusheva, Dan Ferenc Segedin, Berit H. Goodge, Hanjong Paik, Jonathan Pelliciari, Valentina Bisogni, Yanhong Gu, Stefano Agrestini, Abhishek Nag, Mirian García-Fernández, Ke-Jin Zhou, Lena F. Kourkoutis, Charles M. Brooks, Julia A. Mundy, Mark P. M. Dean, and Matteo Mitrano, Magnetic excitations in $Nd_{n+1}Ni_nO_{3n+1}$ Ruddlesden–Popper nickelates observed via resonant inelastic x-ray scattering, Phys. Rev. B **111**, 165145 (2025).

[95] Zhe Liu, Jie Li, Deyuan Hu, Bingke Ji, Haoran Zhang, Jiahao Hao, Yaomin Dai, Qing Li, Mengjun Ou, Bing Xu, Yi Lu, Meng Wang, and Hai-Hu Wen, Highly anisotropic charge dynamics and spectral weight redistribution in the trilayer nickelate $La_4Ni_3O_{10}$, arXiv:2512.03806.

[96] Z. Guan, S. F. R. TenHuisen, M. Tepie, Y. Zhao, E. Day-Roberts, H. LaBollita, A. M. Young, X. Cui, X. Chen, F. Glerean, C. A. Guia, M. P. M. Dean, P. Kim, J. F. Mitchell, A. S. Botana, C. C. Homes, and M. Mitrano, Temperature-dependent infrared optical spectra of $La_4Ni_3O_{10}$ [Data set] Zenodo (2026), 10.5281/zenodo.20089847.